arXiv:1409.5457v1 [cond-mat.str-el] 18 Sep 2014

# Collective Transport Properties of Driven Skyrmions with Random Disorder

C. Reichhardt, D. Ray, and C. J. Olson Reichhardt
*Theoretical Division and Center for Nonlinear Studies,*
*Los Alamos National Laboratory,*
*Los Alamos, New Mexico 87545, USA*

(Dated: September 22, 2014)

We use particle-based simulations to examine the static and driven collective phases of skyrmions interacting with random quenched disorder. We show that non-dissipative effects due to the Magnus term reduce the depinning threshold and strongly affect the skyrmion motion and the nature of the dynamic phases. The quenched disorder causes the Hall angle to become drive-dependent in the moving skyrmion phase, while different flow regimes produce distinct signatures in the transport curves. For weak disorder, the skyrmions form a pinned crystal and depin elastically, while for strong disorder the system forms a pinned amorphous state that depins plastically. At high drives the skyrmions can dynamically reorder into a moving crystal, with the onset of reordering determined by the strength of the Magnus term.

PACS numbers: 75.70.Kw,75.70.Ak,75.85.+t,75.25.-j

There are a wide variety of systems that can be effectively modeled as collectively interacting particles moving over quenched disorder, where there is a transition from a pinned state to a sliding state under an applied drive. Examples include driven incommensurate charge density waves[1,2], Wigner crystals[3,4], colloids driven over various types of substrates[5–7], and vortices in type-II superconductors[8–12]. In many of these systems the particle-particle interactions are repulsive, so that in the absence of disorder a hexagonal crystal of particles forms. When quenched disorder is present, the particles may retain hexagonal or mostly hexagonal order if the disorder is weak, while stronger disorder can lead to a proliferation of topological defects creating an amorphous or glassy state[8,9,13]. If an additional external driving force $F_D$ is now applied to particles in a pinned state, there is a critical drive value $F_c$ known as the depinning threshold above which the particles begin to move. For weak disorder the particles generally depin elastically and retain their original neighbors[1,2,5,7,9], but for strong disorder the depinning is often plastic with particles continuously changing neighbors over time, forming a fluctuating liquid-like state[4–6,9–12]. Additionally, if the depinning occurs from a disordered pinned state, there can be dynamic structural transitions at drives well above $F_c$, where the particles can dynamically order into a moving anisotropic crystal or moving smectic phase[9–11,14–20]. Such transitions occur because the effectiveness of the pinning is reduced in the drive direction when the particles are strongly driven[10]. Transitions from pinned to plastic and from plastic to dynamically ordered states have been observed experimentally through features in transport measures[1,6,9,11], neutron scattering[14], changes in noise fluctuations[11], and direct imaging experiments[18].

Recently a new type of system, skyrmions in chiral magnets, has been realized that can be effectively characterized as particle-like objects interacting with random disorder[21–23]. Neutron scattering experiments showed evidence for triangular skyrmion lattices in bulk MnSi samples[22], and subsequent Lorentz microscopy experiments[22–24] produced direct observations of skyrmion lattices. Imaging measurements indicate that as an externally applied magnetic field is increased, a low-density, partially-disordered skyrmion phase appears out of a helical phase, and is subsequently transformed into a denser ordered triangular lattice of skyrmions; at high fields, the skyrmion number decreases and the system eventually enters a uniform ferromagnetic state[22,23]. In addition to their particle-like nature, another similarity that skyrmions have to vortices in type-II superconductors is that they can be externally driven by the application of a current[25]. Experimental transport measurements have shown[26] that it is possible to obtain skyrmion velocity vs applied driving force curves and that there is a finite depinning threshold. The current-driven motion of skyrmions has also been directly experimentally imaged[27,28].

One aspect of skyrmions that makes them very distinct from other collectively driven systems in random disorder is the pronounced non-dissipative component in the skyrmion equation of motion arising from the Magnus term[23,29–31]. This term causes skyrmions to move in a direction *perpendicular* to the applied driving force, and it has been argued to be the cause of the relatively low depinning threshold observed for skyrmions[23,29–31]. The strength of the Magnus term is denoted by $\beta$ while that of the damping is denoted by $\alpha$. In superconducting vortex systems, $\beta/\alpha \ll 1.0$ so the non-dissipative terms are very weak[8]; in contrast, skyrmion systems typically have $\beta/\alpha$ values ranging from 10 to 40 so that the Magnus term dominates the skyrmion dynamics. This makes skyrmions a unique system in which to explore non-dissipative collective dynamics. Beyond basic science issues, skyrmions may be useful for a range of applications[32] which will require an understanding of skyrmion dynamics in the presence of random disorder.

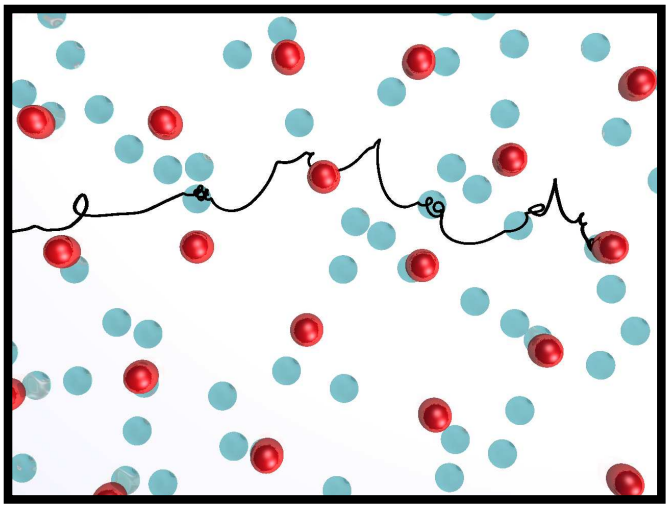

FIG. 1: Real-space image of skyrmions (dark red dots) driven through randomly arranged pinning sites (light blue dots). Here $F_p = 0.03$ and $F_D = 0.0125$; the system is in a moving plastic flow phase. The trajectory of a single moving skyrmion is highlighted, showing spiraling type motions inside the pinning sites.

Here we utilize a recently developed particle-based model for skyrmion dynamics to study collective skyrmion behaviors in the presence of random quenched disorder for varied disorder strengths and varied $\beta/\alpha$ values. We show that the Magnus term reduces the depinning threshold and induces orbits with a circular character for skyrmions moving in and across pinning sites. We also show that collective skyrmion-skyrmion interactions play an important role in the Magnus-induced reduction of the depinning threshold. We find that the Magnus term introduces a Hall angle for the skyrmion motion relative to the direction of the external drive, and that the addition of quenched disorder strongly reduces this Hall angle, particularly just above depinning. At higher drives, the velocity-force curves both parallel and perpendicular to the drive show distinctive features associated with a transition into a dynamically ordered state. We also find disorder-induced transitions from a skyrmion glass to a skyrmion crystal phase, observable as a function of disorder strength or skyrmion density.

*Simulation and System*— We simulate skyrmions interacting with random disorder using a recently developed particle model[31], where the dynamics of a single skyrmion $i$ is governed by the following equation:

$$\alpha\frac{d\mathbf{R}_i}{dt} = \mathbf{F}_i^M + \mathbf{F}_i^{ss} + \mathbf{F}_i^{sp} + \mathbf{F}_i^D. \quad (1)$$

Here $\frac{d\mathbf{R}_i}{dt} = \mathbf{v}_i$ is the skyrmion velocity. The damping term $\alpha$ arises from the damping of the spin precession and damping of electrons localized in the skyrmions. The Magnus term $\mathbf{F}_i^M = \beta\mathbf{v}_i \times \hat{z}$ produces a force oriented perpendicular to the skyrmion velocity. We impose the constraint $\alpha^2 + \beta^2 = 1$ in order to maintain a constant magnitude of the skyrmion velocity for varied ratios of $\beta/\alpha$. For systems such as MnSi, $\beta/\alpha \approx 10$;[31] in this work, unless otherwise noted, we take $\beta/\alpha = 9.962$, corresponding to Magnus-dominated particle dynamics. The skyrmion-skyrmion interaction force is $\mathbf{F}_i^{ss} = \sum_{j=1}^{N_s} \hat{\mathbf{r}}_{ij} K_1(R_{ij})$ where $R_{ij} = |\mathbf{r}_i - \mathbf{r}_j|$, $\hat{\mathbf{r}}_{ij} = (\mathbf{r}_i - \mathbf{r}_j)/R_{ij}$, and $K_1$ is the modified Bessel function which falls off exponentially for large $R_{ij}$. The pinning force $\mathbf{F}_i^{sp}$ arises from randomly placed, non-overlapping harmonic traps of size $R_p = 0.3$ with a maximum pinning force of $F_p$. The driving term $\mathbf{F}^D$ represents a Lorentz force from an externally applied current bias interacting with the emergent magnetic flux carried by the skyrmions[26].

Our system is of size $L \times L$ with $L = 36$, has periodic boundary conditions in the $x$ and $y$ directions, and contains $N_s$ skyrmions and $N_p$ pinning sites. The pin density $\rho_p = N_p/L^2$ is fixed at 0.3, and the skyrmion density $\rho_s = N_s/L^2$ equals 0.1 unless otherwise noted. We apply a slowly increasing driving force $\mathbf{F}^D$ and measure the average skyrmion velocity in the direction parallel (perpendicular) to the applied drive, $\langle V_{\rm drive}\rangle$ ($\langle V_\perp\rangle$). The Hall angle is calculated from these velocities as $\theta = \tan^{-1} R$, where $R = \langle V_\perp\rangle/\langle V_{\rm drive}\rangle$. For a single skyrmion driven in the absence of disorder, $R = \beta/\alpha$, so that $\theta = 84.25°$ for our simulations in the clean limit; in contrast, a vortex with $\beta \approx 0.0$ has $\theta = 0$ and moves along the drive direction.

*Results and Discussion*— In Fig. 1 we show a snapshot of skyrmions moving through random disorder in a small portion of a system with $F_p = 0.03$, and $F_D = 0.01$. Since this drive is well above the depinning threshold $F_c = 0.02$, all the skyrmions are in motion; however, we highlight the trajectory of a single skyrmion, which shows that the skyrmion undergoes a swirling or circular motion within each pinning site it encounters before escaping from the pin. The circular motion arises due to the Magnus term: the force from each pinning site points toward its center, but under Magnus-dominated dynamics this force is largely perpendicular to the skyrmion velocity, causing the skyrmions to circle around the inner edges of the pinning sites. In the overdamped limit with $\beta/\alpha \ll 1$, a skyrmion entering a pinning site would quickly travel to the bottom of the potential well and be strongly pinned. We find that the escape of a skyrmion from a pinning site is strongly affected by motion excited via interactions with the surrounding skyrmions.

We first examine how the Hall angle is affected by the presence of random disorder. To characterize this, in Fig. 2(a) we plot $\langle V_{\rm drive}\rangle$ and $\langle V_\perp\rangle$ versus $F_D$ for a system with $F_p = 0.03$. For $F_D < 0.00625$, the skyrmions are pinned in a disordered arrangement. Just above depinning, $\langle V_{\rm drive}\rangle \approx \langle V_\perp\rangle$, so that $R \approx 1.0$ is much less than the clean-limit value. In general we find that adding quenched disorder decreases $\langle V_\perp\rangle$ and increases $\langle V_{\rm drive}\rangle$ compared to the clean limit, indicating that the average skyrmion flow is rotated back toward the drive direction. This is illustrated in the inset of Fig. 2(a), which shows that the Hall angle is well below the clean-limit value at low drives and approaches it at higher drives. The origin

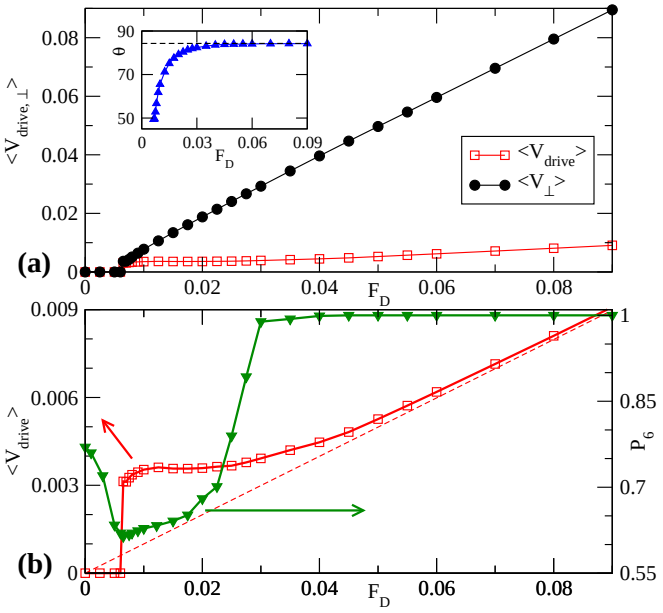


FIG. 2: (a) Average skyrmion velocity in the drive direction, $\langle V_{\rm drive}\rangle$ (open squares), and perpendicular to the drive, $\langle V_\perp\rangle$ (filled circles), vs $F_D$ for system with $F_p = 0.03$. Inset: The Hall angle $\theta$ vs $F_D$; the dotted line is the result for the clean system. (b) $\langle V_{\rm drive}\rangle$ (open squares) and the fraction of six-fold coordinated particles $P_6$ (filled triangles) vs $F_D$ for the same system as in (a); the dashed line shows $\langle V_{\rm drive}\rangle$ for the clean system. There is a dynamical ordering transition into a moving crystal state at $F_D \approx 0.03$.

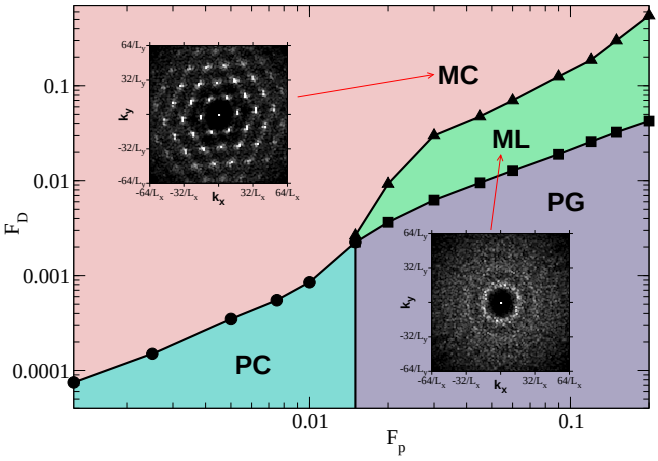


FIG. 3: Dynamical phase diagram for $F_D$ vs $F_p$ highlighting the different skyrmion phases. PC: pinned crystal; PG: pinned amorphous glass; ML: moving liquid; MC: moving crystal. Circles: elastic depinning from PC to MC; squares: plastic depinning from PG to ML; triangles: dynamical ordering transition from ML to MC. Upper inset: structure factor $S(k)$ of the skyrmion positions in the MC state. Lower inset: $S(k)$ in the ML state.

of this behavior is a ratcheting effect experienced by the skyrmions as they encounter pinning sites. When a drive is applied, the equilibrium pinned position of a skyrmion is displaced from the pin's center in the direction of the drive, and a skyrmion driven over a pin will be pulled toward this equilibrium point. Consequently, on average, the outgoing trajectory of a skyrmion emerging from a pin is offset in the drive direction relative to its incoming trajectory. When $F_D \lesssim F_p$, a skyrmion can spend a lot of time interacting with a pinning site, enhancing the size of this offset, while for higher drives the offset is diminished.

At the drive value shown in Fig. 1, the skyrmions form a disordered state; however, at higher drives they can dynamically order into a moving crystal. In Fig. 2(b) we plot the fraction of six-fold coordinated particles $P_6$ as a function of $F_D$ along with $\langle V_{\rm drive}\rangle$ for the same system as in Fig. 2(a). $P_6$ is smallest right at depinning where the particles are most disordered, but rapidly approaches 1 around $F_D \approx 0.025$ indicating dynamical reordering of the system. Simultaneously, $\langle V_{\rm drive}\rangle$ acquires a linear dependence on $F_D$, with values approximating the clean-limit value.

In Fig. 3 we plot a dynamical phase diagram highlighting the static and dynamic phases for skyrmions as $F_D$ and $F_p$ are varied. For $F_p < 0.015$ the skyrmions form a pinned triangular crystal (PC) which depins elastically to a moving crystal state (MC) as the drive increases. For $F_p > 0.015$ at low drives, we instead find an amorphous pinned skyrmion glass (PG) which depins *plastically* with increasing drive into a fluctuating moving skyrmion liquid (ML). The lower inset of Fig. 3 shows that the structure factor $S(k)$ of the ML phase has a liquid-like ring. As $F_D$ increases further, the moving liquid transitions into a moving skyrmion crystal state with sixfold ordering, as shown in the plot of $S(k)$ in the upper inset of Fig. 3. This phase diagram has similarities to that found for a driven vortex system[19]; however, the skyrmions reorder into a moving crystal rather than a moving smectic state. The vortex moving smectic state forms when the pinning remains effective in the direction transverse to the vortex motion while being weakened in the direction of motion, subjecting the vortices to an effective anisotropic temperature. In the skyrmion case, additional fluctuations induced by the Magnus force reduce the transverse pinning in the moving state, giving a more isotropic effective temperature and allowing the skyrmions to form a more isotropic moving structure. We expect that neutron scattering experiments could be used to observe the transition from a skyrmion glass to a moving skyrmion crystal state as a function of external drive.

To better understand how the pinning affects skyrmion motion, in Fig. 4(a) we plot $\langle V_{\rm drive}\rangle$ and $\langle V_\perp\rangle$ for fixed $F_D = 0.0075$ and varied pinning strength. As $F_p$ increases and the skyrmions transition from MC to ML to PG (as shown in Fig. 3), $\langle V_{\rm drive}\rangle$ increases and $\langle V_\perp\rangle$ decreases from the clean-limit values so that $\langle V_{\rm drive}\rangle$ actually slightly exceeds $\langle V_\perp\rangle$ at $F_p = 0.035$, just before the skyrmions become pinned. The Hall angle accordingly decreases as $F_p$ is increased. In Fig. 4(b) we plot

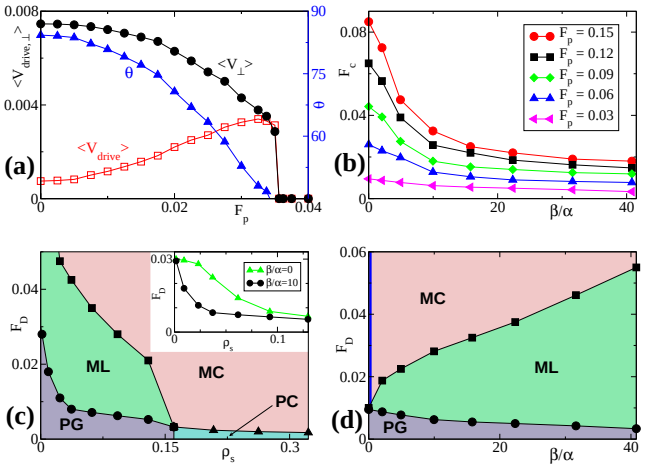


FIG. 4: (a) $\langle V_{\rm drive}\rangle$, $\langle V_\perp\rangle$, and $\theta$ as a function of disorder strength $F_p$, at fixed drive $F_D = 0.0075$. (b) The critical depinning force $F_c$ vs $\beta/\alpha$ for $F_p = 0.15$, 0.12, 0.09, 0.06, and 0.03, from top to bottom. (c) Phase diagram for $F_D$ vs $\rho_s$ at $F_p = 0.03$, highlighting the transition from PG to ML (circles), ML to MC (squares), and PC to MC (triangles). Inset: The depinning threshold (PG-ML transition line) for Magnus-dominated (circles) and damping-dominated (triangles) particle dynamics. (d) Phase diagram of $F_D$ vs $\beta/\alpha$ for $F_p = 0.03$, showing transitions from PG to ML (circles) and ML to MC (squares). Blue line along upper left axis indicates moving smectic state for overdamped particles.

the critical depinning force $F_c$ vs $\beta/\alpha$ for varied $F_p$. As the dynamics become increasingly Magnus-dominated for higher $\beta/\alpha$, $F_c$ monotonically decreases, confirming that inclusion of Magnus forces lowers the depinning threshold. This effect is more prominent for higher values of $F_p$.

In Fig. 4(c) we plot the phase diagram for $F_D$ versus skyrmion density $\rho_s$ at fixed $F_p = 0.03$. At low skyrmion densities, a disordered pinned state forms that depins plastically into a moving liquid and then orders into a moving crystal at higher drives; at higher $\rho_s$, we find a pinned crystal state that depins elastically directly into a moving crystal state. Notably, the depinning threshold is very close to $F_p$ at the lowest simulated density (near the single skyrmion limit), but falls off rapidly as $\rho_s$ increases. This indicates that *collective* skyrmion-skyrmion interactions play a crucial role in producing a low depinning threshold. This is further emphasized in the inset of Fig. 4(c) where we show how the plastic depinning line is altered when we go from Magnus-dominated to damping-dominated particle dynamics. At low $\rho_s$, $F_c$ is nearly the same for the two systems; however, once the skyrmion-skyrmion interactions become important for higher $\rho_s$, the falloff in the depinning threshold with increasing $\rho_s$ is much more rapid in the Magnus-dominated system. In Fig. 4(d) we show how the dynamical phase diagram changes as the dynamics become increasingly Magnus-dominated by plotting the phases as a function of $F_D$ and $\beta/\alpha$. When $\beta/\alpha = 0$, the behavior is the same as that of a vortex system and the system reorders into a moving smectic rather than a moving crystal. As $\beta/\alpha$ increases, the depinning threshold drops while the drive at which dynamical reordering occurs increases due to the enhanced swirling motion of the skyrmions in the liquid state, which produces an effective temperature that is more isotropic but also larger in magnitude compared to the overdamped case.

*Summary*— We have investigated the depinning dynamics of skyrmions interacting with random disorder, utilizing a recently developed particle-based skyrmion model. We find that the Magnus-dominated dynamics typical of skyrmions decreases the depinning threshold due to the swirling orbits followed by skyrmions interacting with pinning sites. Skyrmion-skyrmion scattering tends to excite such orbits and thus also plays an important role in reducing the depinning threshold. For increasing disorder strength we find transitions from a pinned skyrmion crystal to an amorphous skyrmion glass. We also show that the Hall angle deviates from its clean-limit value for strong pinning or weak driving. At high drives, in contrast to superconducting vortices which dynamically reorder into a smectic state, the skyrmions undergo a dynamical phase transition from a fluctuating driven liquid to a moving crystal. This occurs because the Magnus term tends to make the fluctuations, and the resulting effective temperature, experienced by the skyrmions more isotropic with respect to the direction of the external drive compared to a damping-dominated system. Features in the transport response such as velocity-force curves or structure factor measurements can be used to identify signatures of the different dynamical phases.

### Acknowledgments

We thank S.-Z. Lin for useful discussions. This work was carried out under the auspices of the NNSA of the U.S. DoE at LANL under Contract No. DE-AC52-06NA25396 and through the LANL/LDRD program.

[1] G. Grüner, Rev. Mod. Phys. **60**, 1129 (1988).
[2] L. Balents and M.P.A. Fisher, Phys. Rev. Lett. **75**, 4270 (1995).
[3] F.I.B. Williams *et al.*, Phys. Rev. Lett. **66**, 3285 (1991).
[4] M.-C. Cha and H.A. Fertig, Phys. Rev. B **50**, 14368 (1994).
[5] C. Reichhardt and C. J. Olson, Phys. Rev. Lett. **89**, 078301 (2002).
[6] A. Pertsinidis and X.S. Ling, Phys. Rev. Lett. **100**, 028303 (2008).
[7] T. Bohlein, J. Mikhael, and C. Bechinger, Nature Mater.

**11**, 126 (2012).
[8] G. Blatter, M.V. Feigelman, V.B. Geshkenbein, A.I. Larkin, and V.M. Vinokur, Rev. Mod. Phys. **66**, 1125 (1994).
[9] S. Bhattacharya and M.J. Higgins, Phys. Rev. Lett. **70**, 2617 (1993).
[10] A.E. Koshelev and V.M. Vinokur, Phys. Rev. Lett. **73**, 3580 (1994).
[11] A.C. Marley, M.J. Higgins, and S. Bhattacharya, Phys. Rev. Lett. **74**, 3029 (1995).
[12] Y. Fily, E. Olive, N. Di Scala, and J.C. Soret, Phys. Rev. B **82**, 134519 (2010).
[13] M.-C. Cha and H.A. Fertig, Phys. Rev. Lett. **74**, 4867 (1995).
[14] U. Yaron *et al.*, Nature (London) **376**, 753 (1995).
[15] K. Moon, R.T. Scalettar, and G.T. Zimányi, Phys. Rev. Lett. **77**, 2778 (1996).
[16] T. Giamarchi and P. Le Doussal, Phys. Rev. Lett. **76**, 3408 (1996); P. Le Doussal and T. Giamarchi, Phys. Rev. B **57**, 11356 (1998).
[17] L. Balents, M.C. Marchetti, and L. Radzihovsky, Phys. Rev. B **57**, 7705 (1998).
[18] F. Pardo, F. de la Cruz, P.L. Gammel, E. Bucher, and D.J. Bishop, Nature (London) **396**, 348 (1998).
[19] C.J. Olson, C. Reichhardt, and F. Nori, Phys. Rev. Lett. **81**, 3757 (1998).
[20] H. Fangohr, S.J. Cox, and P.A.J. de Groot, Phys. Rev. B **64**, 064505 (2001).
[21] S. Mühlbauer, B. Binz, F. Jonietz, C. Pfleiderer, A. Rosch, A. Neubauer, R. Georgii, and P. Böni, Science **323**, 915 (2009).
[22] X.Z. Yu, Y. Onose, N. Kanazawa, J.H. Park, J.H. Han, Y. Matsui, N. Nagaosa, and Y. Tokura, Nature (London) **465**, 901 (2010).
[23] N. Nagaosa and Y. Tokura, Nature Nanotechnol. **8**, 899 (2013).
[24] X.Z. Yu, N. Kanazawa, Y. Onose, K. Kimoto, W.Z. Zhang, S. Ishiwata, Y. Matsui, and Y. Tokura, Nature Mater. **10**, 106 (2011).
[25] F. Jonietz, S. Mühlbauer, C. Pfleiderer, A. Neubauer, W. Münzer, A. Bauer, T. Adams, R. Georgii, P. Böni, R.A. Duine, K. Everschor, M. Garst, and A. Rosch, Science **330**, 1648 (2010).
[26] T. Schulz, R. Ritz, A. Bauer, M. Halder, M. Wagner, C. Franz, C. Pfleiderer, K. Everschor, M. Garst, and A. Rosch, Nature Phys. **8**, 301 (2012).
[27] X.Z. Yu, N. Kanazawa, W.Z. Zhang, T. Nagai, T. Hara, K. Kimoto, Y. Matsui, Y. Onose, and Y. Tokura, Nature Commun. **3**, 988 (2012).
[28] X.Z. Yu, Y. Tokunaga, Y. Kaneko, W.Z. Zhang, K. Kimoto, Y. Matsui, Y. Taguchi, and Y. Tokura, Nature Commun. **5**, 3198 (2014).
[29] J. Iwasaki, M. Mochizuki, and N. Nagaosa, Nature Commun. **4**, 1463 (2013).
[30] J. Iwasaki, M. Mochizuki, and N. Nagaosa, Nature Nanotechnol. **8**, 742 (2013).
[31] S.-Z. Lin, C. Reichhardt, C.D. Batista, and A. Saxena, Phys. Rev. B **87**, 214419 (2013).
[32] A. Fert, V. Cros, and J. Sampaio, Nature Nanotechnol. **8**, 152 (2013).